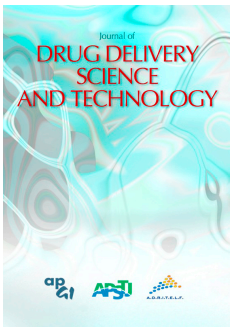


# 18-β-Glycyrrhetinic acid encapsulated PLGA nanoparticles attenuate lung cancer proliferation and migration

Keshav Raj Paudel, Mohamad Siddiq Bin Mohamad, Gabriele De Rubis, Ruby-Jean Reyes, Nisha Panth, Harish Dureja, Gaurav Gupta, Sachin Kumar Singh, Thiagarajan Madheswaran, Trudi Collet, Philip Michael Hansbro, Kamal Dua, Dinesh Kumar Chellappan

PII: S1773-2247(24)00191-6

DOI: https://doi.org/10.1016/j.jddst.2024.105523

Reference: JDDST 105523

To appear in: *Journal of Drug Delivery Science and Technology*

Received Date: 10 June 2023

Revised Date: 11 February 2024

Accepted Date: 28 February 2024

Please cite this article as: K.R. Paudel, M.S.B. Mohamad, G. De Rubis, R.-J. Reyes, N. Panth, H. Dureja, G. Gupta, S.K. Singh, T. Madheswaran, T. Collet, P.M. Hansbro, K. Dua, D.K. Chellappan, 18-β-Glycyrrhetinic acid encapsulated PLGA nanoparticles attenuate lung cancer proliferation and migration, *Journal of Drug Delivery Science and Technology* (2024), doi: https://doi.org/10.1016/j.jddst.2024.105523.

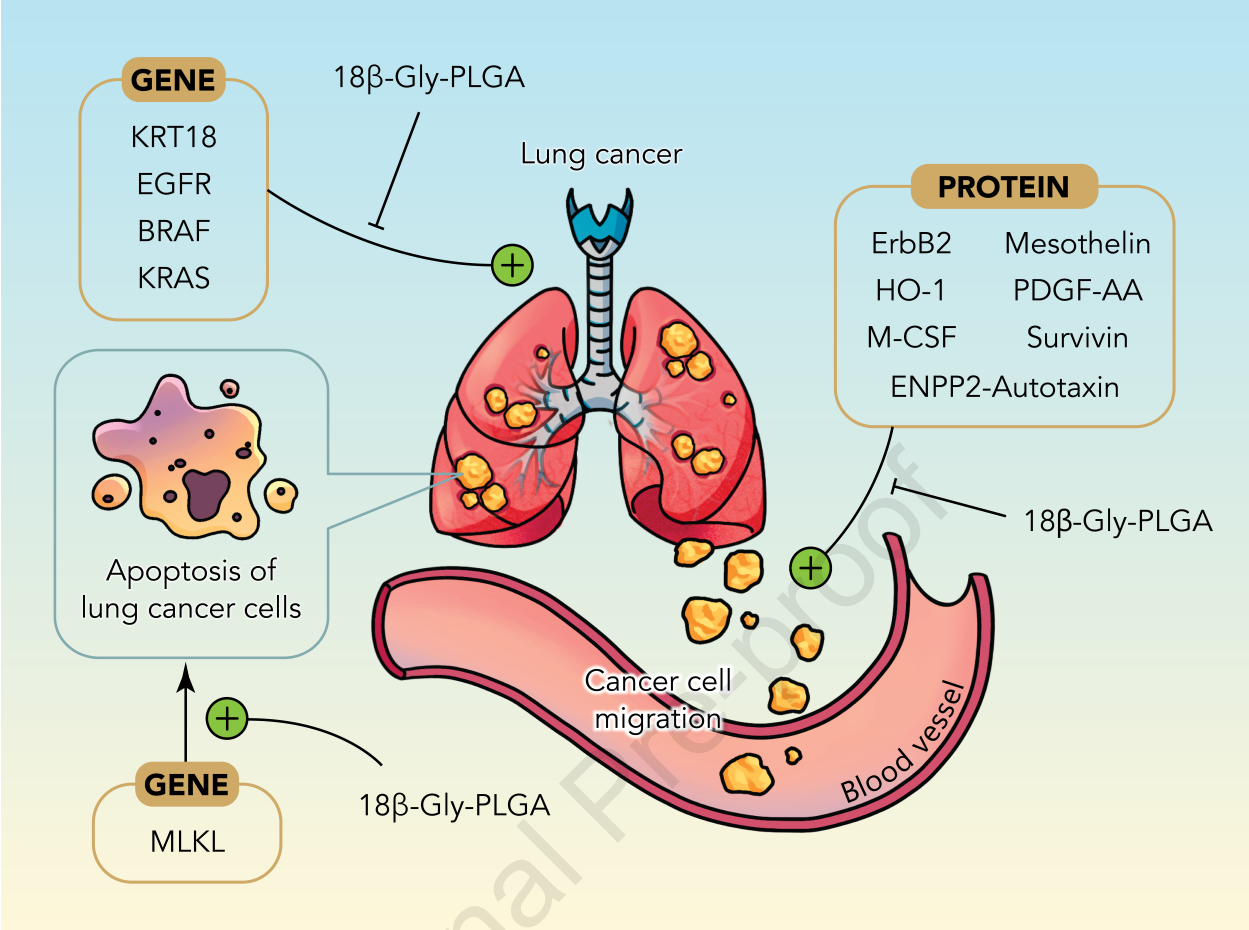

# 18-β-Glycyrrhetinic acid encapsulated PLGA nanoparticles attenuate lung cancer proliferation and migration

Keshav Raj Paudel[1,#], Mohamad Siddiq Bin Mohamad[2,3,#], Gabriele De Rubis[3,4], Ruby-Jean Reyes[3,4], Nisha Panth[1], Harish Dureja[5], Gaurav Gupta[6,7,8], Sachin Kumar Singh[3,9], Thiagarajan Madheswaran[10], Trudi Collet[11], Philip Michael Hansbro[1,*], Kamal Dua[3,4,**], Dinesh Kumar Chellappan[12,***]

[1]Centre for Inflammation, Centenary Institute and University of Technology Sydney, Faculty of Science, School of Life Sciences, Sydney, Australia 2007

[2]School of Postgraduate Studies, International Medical University, Bukit Jalil 57000, Kuala Lumpur, Malaysia

[3]Faculty of Health, Australian Research Centre in Complementary & Integrative Medicine, University of Technology Sydney, Ultimo, Australia 2007

[4]Discipline of Pharmacy, Graduate School of Health, University of Technology Sydney, Sydney, NSW, Australia 2007

[5]Department of Pharmaceutical Sciences, Maharshi Dayanand University, Rohtak 124001, Haryana, India

[6]School of Pharmacy, Suresh Gyan Vihar University, Mahal Road, Jagatpura, Jaipur, India

[7]Department of Pharmacology, Saveetha Dental College & Hospitals, Saveetha Institute of Medical & Technical Sciences, Saveetha University, Chennai, India

[8]Uttaranchal Institute of Pharmaceutical Sciences, Uttaranchal University, Dehradun, India

[9]School of Pharmaceutical Sciences, Lovely Professional University, Phagwara, Punjab, 144411, India

[10]Department of Pharmaceutical Technology, School of Pharmacy, International Medical University, Bukit Jalil 57000, Kuala Lumpur, Malaysia.

[11]Innovative Medicines Group, Faculty of Health, Queensland University of Technology, Kelvin Grove, QLD, Australia 4059.

[12]Department of Life Sciences, School of Pharmacy, International Medical University, Bukit Jalil 57000, Kuala Lumpur, Malaysia.

*Corresponding author: Prof Philip Michael Hansbro; E-mail: Philip.Hansbro@uts.edu.au
**Corresponding author: Dr Kamal Dua; E-mail: Kamal.Dua@uts.edu.au
***Corresponding author: Dr Dinesh Kumar Chellappan; E-mail: Dinesh_Kumar@imu.edu.my
#Equal contribution

**Abstract**

Conventional treatment methods to treat lung cancer include radiation therapy, chemotherapy, and immunotherapy. However, they cause severe adverse effects and recurrence risk. 18-β-glycyrrhetinic acid (18-β-Gly), a naturally occurring bioactive compound extracted from the liquorice plant has demonstrated anticancer potential by suppressing cancer cell growth, angiogenesis, and metastasis. Although 18-β-Gly possesses potential therapeutic abilities, the application of 18-β-Gly into clinical practices is hindered due to its inferior physicochemical characteristics such as poor bioavailability and low water solubility. Poly lactic-*co*-glycolic acid (PLGA) is a synthetic polymer with great tuneable options for a nano-drug delivery system used for various diseases, including cancer. Formulating 18-β-Gly into PLGA has helped to overcome challenges imposed by the poor physicochemical characteristics of 18-β-Gly. For this research, 18-β-Gly-PLGA was tested for its anticancer ability using A549 human lung adenocarcinoma lines found in lung cancer. Findings showed that 18-β-Gly-PLGA has favourable physicochemical characteristics, such as sustained *in vitro* drug release and good entrapment efficiency. 18-β-Gly-PLGA was also able to inhibit 15% and 50% proliferation of A549 cells at 2.5μM and 50μM respectively and 28% inhibition of A549 cell migration at 5μM concentration. Oncogenes such as *KRT18, EGFR, BRAF* and *KRAS* were significantly downregulated by 43%, 19.3%, 14.7% and 13.7% respectively as part of the anticancer effects and the underlying mechanism of 18-β-Gly-PLGA. Significant reduction in the expression of cancer proliferation and migration-associated proteins such as receptor tyrosine-protein kinase ErbB2, survivin, macrophage colony-stimulating factor and mesothelin was also observed. The findings of this study demonstrate the promising potential of 18-β-Gly-PLGA as a potential anticancer agent.

**Keywords:** 18-β-Glycyrrhetinic acid, PLGA nanoparticle, non-small-cell lung cancer, A549 lung cancer cells, mRNA expression, protein expression

## 1. INTRODUCTION

Lung cancers are the leading cause of malignancy-related morbidity and mortality globally [1]. Small-cell lung cancer (SCLC) and non-small cell lung cancer (NSCLC) are two subtypes of lung cancer based on cell origin [2]. In 2018, GLOBOCAN data indicated that globally, lung cancers have the highest incidence among all other cancers with 2,094,000 new cases reported. Lung malignancy caused approximately 1.76 million deaths worldwide in 2018, or put simply, 18.4% of all cancer-related deaths [3]. In men with a history of cigarette smoking, lung cancers are common and they have a higher risk of developing lung cancer than females [4]. Women and individuals without a history of smoking are more likely to develop adenocarcinoma, which is characterised by the tumor being located at the lung periphery and the presence of targetable driver mutations in the epidermal growth factor receptor (*EGFR*), anaplastic lymphoma kinase (*ALK*), B-type rapidly accelerated fibrosarcoma (RAF) kinase (*BRAF*), and ROS proto-oncogene 1, receptor tyrosine kinase (*ROS1*) genes [5].

The multiple underlying mechanisms through which lung cancer forms involves several genetic and epigenetic alterations, most notably the activation of tumor-promoting pathways and the suppression of tumor-suppressor pathways [6]. Lung cancer tumorigenesis, like other cancers, is linked to the activation of growth-promoting proteins such as v-Ki-ras2 Kirsten rat sarcoma viral oncogene homolog (*KRAS*), *EGFR*, *BRAF*, mitogen-activated protein kinase kinase-1 (*MEK-1*), ErbB2 receptor tyrosine kinase 2 (*HER2*), receptor tyrosine kinase **(***MET*), MET proto-oncogene, *ALK*, and rearranged during transfection (*RET*) as well as the inactivation of tumour suppressor genes such as tumor protein p53 (*p53*), phosphatase with tensin homology (*PTEN*) and serine/threonine kinase 11 (*LKB-1*) [6-10]. Keratin 18 (*KRT18*) has been proposed to play an important part in the signalling pathway that regulates important cellular activities

such as growth, motility and death [11]. The upregulation of *KRT18* is significantly linked to poor prognosis, recurrence, lymph node metastasis as well as distant metastasis [11].

Lung cancer cell proliferation and migration also involve over-expression of several proteins such as ErbB2, heme oxygenase-1 (HO-1), macrophage colony stimulating factors (M-CSF), mesothelin, platelet derived growth factor AA (PDGF-AA) and survivin. ErbB2, a tyrosine kinase receptor which is involved in cell proliferation, is over-expressed in lung cancer [12]. HO-1 overexpression is mainly seen in NSCLC where the protein enhances migration and invasiveness ability of cancer cells when exposed to high sugar level [13]. M-CSF commonly seen in lung cancer cells, plays a significant role in stimulating tumour invasion [14]. Mesothelin is greatly involved in epithelial to mesenchymal transition (EMT) and stemness in lung cancer [15]. PDGF-AA is a protein which regulates expression of vascular endothelial growth factor (VEGF) and the overexpression of this protein is important for cancer angiogenesis [16]. Survivin, a type of protein involved in preventing apoptosis, is crucial in cancer cell proliferation [17]. ENNP2-Autotaxin is a secreted glycoprotein that catalyses the extracellular production of lysophosphatidic acid (LPA). The over-expression of this protein is related to an increase in angiogenesis and metastasis [7]. One of the strategies to control cancer cell proliferation is by inducing cell death through apoptosis or necroptosis pathway [18, 19]. Among death-receptor-induced necroptosis, the protein kinase receptor interacting protein kinase 1, 3 (RIPK1, RIPK3) and the mixed lineage kinase domain-like (MLKL) constitute the core part of necroptosis pathway [19]. RIPK function has a crucial role in different pathways of death receptor signalling, such as the activation of NF-κB and MAP (mitogen activated protein) kinases, and the induction of apoptosis and necroptosis [19]. We have previously shown that NF-κB decoy oligonucleotide possess antiproliferative activity against lung cancer cells by inducing apoptosis through overexpression of *RIPK1*, *RIPK3*, and *MLKL* gene [20]. Thus, an ideal medication should target the aforementioned cell signalling pathway involved

in cancer progression as such as cancer cell proliferation, migration, survival, apoptosis, and angiogenesis.

Currently, there is a lack of medications that can absolutely cure lung cancer, although the treatments that are available mostly target neoplastic cells at the proliferation and migration level [21]. Chemotherapy, radiotherapy, and immunotherapy are the main types of treatment [22]. However, their usage is restricted because of the numerous associated side effects and the issue of affordability due their high cost. In light of this, researchers are constantly looking for novel therapeutic approaches that can slow down and, ideally, mitigate and halt the progression of lung cancer. Numerous phytoceuticals elicit strong *in vitro* anti-cancer activity and include berberine [23-28], curcumin [29], rutin [30], naringenin [31], boswellic acid [32], nobiletin [33], zerumbone [34], as well as plant extracts such as agarwood oil [35] and polyherbal formulation [36]. Another promising phytoceutical that demonstrates great potential as an anti-cancer agent is 18-β-glycyrrhetinic acid (18- β-Gly) [37]. 18-β-Gly, originally extracted from glycyrrhizic acid/glycyrrhizin from the liquorice plant, has been used in traditional medicine for centuries due to its therapeutic effects [38]. 18-β-Gly possesses beneficial attributes such as anti-neoplastic, anti-inflammatory, anti-oxidant, and anti-bacterial properties [39-41]. However, despite all the potential shown by 18-β-Gly, it has some undesirable physicochemical properties which include poor bioavailability and low water solubility, thereby restricting its therapeutic application [42]. As such, physiochemical parameter enhancement strategies are needed to improve the bioavailability of 18-β-Gly. Therefore, the rationale for encapsulating 18-β-Gly acid into poly lactic-*co*-glycolic acid (PLGA) nanoparticles is to overcome all these physiochemical hurdles and to enhance its biological activity.

In recent years, there is increasing interest in utilising nanotechnology to overcome the challenges that are brought by nutraceuticals [43, 44]. The benefits of using nanocarriers include safely carrying bio-active compounds without affecting pharmacological effects that

these compounds might possess while simultaneously improving the bio-active physicochemical characteristics [45]. Other advantages of utilising functional nanoparticles include improving the stability of the compound *in vivo* [46, 47]. There are three categories of nanomaterials which include polymeric, lipid-based as well as inorganic nanocarriers. Polymeric micelles, polymersomes, polymeric nanogels, polymeric nanocapsules and dendrimers are examples of polymeric nanocarriers (PNCs) [48, 49]. The United States Food and Drug Administration (FDA) has generally deemed the synthetic polymer, (PLGA) to be safe for use in drug nano-formulations for the treatment of pulmonary diseases [50]. When creating nanodrug delivery systems to remedy various ailments, PLGA is commonly the material of choice. PLGA particles are used in the treatment of cancer [51], diabetes [52], prevention of infections [53], and as anti-inflammatory [54]. Water and carbon dioxide are the main PLGA by-products, and these substances are quickly eliminated *via* the body's citric acid cycle [55]. Favourable biocompatibility, biodegradable nature, adaptive degradation, and controllable mechanical properties are just a few of the advantageous characteristics that PLGA demonstrates. Surface modification can alter the hydrophobic properties of PLGA, enhancing the biological activity of the formulations. When employed in animal models, drug-loaded PLGA nanoparticles showed good stability and sustained drug concentration in the blood for a longer period of time [56]. PLGA nanoparticles have the potential to treat a number of lung disorders in an efficient manner.

In this study, the first aim was to encapsulate 18-β-Gly using PLGA to prepare nano-formulations. The prepared nano-formulation was characterized for specific physicochemical parameters which include particle size, zeta potential, polydispersity index, entrapment efficiency, and *in vitro* release. The second aim was to test the *in vitro* efficacy of 18-β-Gly nano-formulation against human lung adenocarcinoma cell lines (A549). This study shows the huge potential of 18-β-Gly as a viable option for lung cancer treatment.

## 2. MATERIALS AND METHODS

### Chemicals and Reagents

MTT (3-[4,5-dimethylthiazol-2-yl]-2,5-diphenyl tetrazolium bromide), Dulbecco's Modified Eagle's Medium (DMEM) media, antibiotics mix (10,000 unit/ml of penicillin and 10 mg/ml of streptomycin), phosphate buffer saline (PBS), trypsin, reagents related with RNA extraction, cDNA synthesis, crystal violet, dimethyl sulfoxide (DMSO) and hematoxylin/eosin (H/E) staining solutions were purchased from Sigma-Aldrich, Missouri, St. Louis, United States of America (USA). Proteome Profiler Human XL oncology array kit was purchased from R&D systems, Inc. a Bio-Techne brand (Minneapolis, USA). 18-β-Gly, 97%, Resomer RG 504 H (PLGA), Resomer RG 752 H (PLGA), dichloromethane (99.8%), acetone (99.9%) and poloxamer 407 were procured from Sigma-Aldrich, Missouri, St. Louis, United States of America (USA). In this investigation, all the solvents and reagents utilized were analytical research grade.

### Solubility analysis

For the solubility analysis, 10 mg of 18-β-Gly was added to 1mL of methanol to obtain a concentration of 10000 µg/mL. This was then further diluted with methanol to obtain concentrations of 10, 20, 40, 60, and 80 µg/mL. The soluble 18-β-Gly concentration in these samples were determined by measuring their absorbance at a wavelength (λ) of 248nm using the UV-visable spectroscopy. The optical density (OD) values of the samples were then plotted against their concentration and the $R^2$ value (greater than 0.99) and the graph equation was calculated.

### Preparation of 18-β-Gly encapsulated PLGA nanoparticles

Nanoparticles were synthesized using the adapted emulsion-evaporation method [57]. Five mL of dichloromethane and acetone (dichloromethane/acetone 3/2) were used to dissolve 50 mg of

PLGA to produce a well-mixed PLGA solution (10 mg/mL) as PLGA completely dissolved. 10 mg of 18-β-Gly was added into the PLGA solution and sonicated at room temperature for 2 min at 200 W (organic phase) to develop a primary emulsion. The primary emulsion was slowly added into the Poloxamer solution (1 percent w/v) (aqueous phase), with a further 4 minutes of sonication room temperature at 200 W, which formed the final oil/water (O/W) emulsion. 15 mL deionized water were added to disseminate the final O/W emulsion. Centrifugation at 14,000 rpm at room temperature for 30 minutes helped extract the nanoparticles with also the supernatant removed. The nanoparticles obtained were centrifuged three times for 20 minutes at 10,000 rpm at room temperature with the deionized water removed. The nanoparticles were then freeze-dried -20 °C and deposited at 4 °C after being vacuum frozen and resuspended in deionized water. By using dynamic light scattering (DLS), the physicochemical characteristics of 18-β-Gly-encapsulated PLGA nanoparticles were confirmed [57].

**Physicochemical characterization**

**Particle size, polydispersity index (PDI), zeta potential and morphological analysis**

Using Zetasizer, the prepared nano-formulations' crucial physicochemical parameter namely, particle size, zeta potential and polydispersity index (PDI) were assessed. Prior to analysis, 20 times dilution done using distilled water and the measurement taken in triplicate [58].

The morphology of 18-β-Gly-encapsulated PLGA nanoparticles was investigated using a Hitachi TM3000 scanning electron microscope (SEM) operating at an accelerating voltage of 15 kV. For this analysis, a small quantity of the 18-β-Gly-PLGA nanoparticles was spread onto double-sided tape secured to an aluminium stub.

**Entrapment efficiency (EE)**

500 µL of 18-β-Gly-encapsulated PLGA nanoparticles underwent centrifugation at 2,500×g for 15 minutes at room temperature in a centrifugal filter. Before analysis, a 10-fold dilution of

the whole centrifuged filtrate (30 µL) was prepared. Furthermore, 100 µL containing 18-β-Gly-encapsulated PLGA nanoparticles also underwent 10-times dilution in methanol. By using UV-visible spectroscopy at 248nm, the total concentration of 18-β-Gly in and the concentration of free 18-β-Gly were calculated. Each measurement was acquired in three replicates and the EE was computed using the following equation.:

$$EE = \frac{\text{Total } 18\beta\text{−GLY concentration} - \text{Total free } 18\beta\text{−GLY}}{\text{Total } 18\beta\text{−GLY concentration}} \times 100\%$$

where entrapment efficiency is denoted by EE.

***In vitro* release study**

To determine the *in vitro* release patterns of the formulations, the dialysis method was used. A Spectra/Por dialysis membrane bag with a molecular weight cut-off of 3500 g/mol was used to hold 1 ml of 18-β-Gly-encapsulated PLGA nanoparticles (containing 1.5 mg of 18-β-Gly) dispersed in 0.01 M phosphate buffer, pH 7.4 and free 18-β-Gly (1.5 mg of 18-β-Gly dissolved in 20% ethanol). The dialysis bag was then placed in 20 mL of 10% ethanol in 0.01 M phosphate buffer, pH 7.4 in a falcon tube. Concurrently, the entire setup was shaken at 70 strokes per minute with the temperature maintained at 37°C in a water bath. The 1 mL sample was removed from the tube and analysed at various time intervals, *i.e.* 0.5, 1, 2, 3, 6, 9, 12, and 24 hours. An equal amount of fresh release medium was reintroduced back into the tube after each withdrawal. The amount of 18-Gly released was measured at 248 nm using UV-visible spectroscopy.

**Cell Culture**

For *in vitro* experiments, human lung carcinoma A549 cells (ATCC, Manassas, VA, USA) received from Prof. Alaina Ammit (Woolcock Institute of Medical Research, Sydney, Australia) were used and grown in Dulbecco's Modified Eagle's Medium (DMEM)

supplemented with 5-10% foetal bovine serum, 1% antibiotic mix (penicillin and streptomycin) in humidified 5% $CO_2$ incubator at 37 °C. 18-β-Gly-PLGA or empty NP were treated to A549 cells at the given concentrations for 24 hours below to conduct the *in vitro* tests.

**Cell viability assay**

The % of viable A549 cells was assessed using the MTT assay in response to 24 hours treatment of 18-β-Glycyrrhetinic acid-encapsulated PLGA nanoparticles as previously described by Paudel et al. [59]. First, a 96-well plate was used to seed the A549 cells. These cells treated with 18-β-Glycyrrhetinic acid-encapsulated PLGA nanoparticles for 24 hours. Each well received a final dose of 0.5 mg/ml of the MTT solution before being incubated at 37 °C for 4 hours. The supernatant layer will be delicately removed in the next phase. The mixture will then be accurately dosed with 100 µl of dimethyl sulphoxide (DMSO), which will dissolve the formazan crystals that have formed. At 540 nm, the absorbance of the resulting purple chromophore was measured. Cells in the untreated group (control) will set at 100% viability rate. However, the cells treated with 18-β-Glycyrrhetinic acid-encapsulated PLGA nanoparticles will be used to calculate the % viability.

**Colony forming assay**

Colony forming assay was carried out as previously reported [23]. A549 cells were plated in 6-well plates at low density of 500 cells per well and cultivated for up to two weeks at a constant temperature of 37 °C in the presence or absence of 18-β-Gly-PLGA or empty nanoparticles (NP) with media replaced every 48 hours. After cells being washed with PBS, the cells were fixed for 20 minutes at room temperature with 3.7% (v/v) formaldehyde. After being stained with 0.4% crystal violet solution, the cells were washed with PBS. The six well plates were photographed from the bottom side.

**Wound healing assay**

Wound healing migration assays were utilized to assess the influence of 18-β-Gly-PLGA and empty NP on A549 cell migration [24]. $2.5\times10^5$ A549 cells/well were seeded in 6-well plates. Next day, using the tip of a sterile 200 µL pipette, a scratch was made on the cell monolayer. The cells were grown at 37 °C for 24 hours under 5% $CO_2$ with 18-β-Gly-PLGA or with empty NP after being washed with PBS to eliminate floating cells. During zero and 24 hours of incubation, pictures were acquired using a phase contrast microscope with a 10-objective lens. A percentage (%) of the difference in wound width from zero to 24 hours relative to zero hour was used to compute wound closure.

**Trans-well chamber migration assay**

In a 48-well plate, A549 cells were seeded at a density of 20,000 cells per well (Corning). The cells were cultured at 37 °C for 24 hours under 5% $CO_2$ with or without 18-β-Gly-PLGA (final concentrations of 5 µM) after 80% confluency. Cells were trypsinised and then washed once with PBS and centrifuged at 300x g for four minutes at room temperature. Next, the supernatant was decanted, and PBS was used to resuspend the cell pellets. In the subsequent steps, trypan blue solution (0.4% (w/v) (Thermo Fisher Scientific, Waltham, MA, USA) was mixed 1:1 with 10 µL of cell suspension. Viable cells number were then determined using a hemacytometer (Hawksley and Sons Ltd., Lancing, UK) and a phase-contrast microscope as previously described [23].

**Reverse transcriptase-quantitative polymerase chain reaction (RT-qPCR)**

A549 cells in the presence or absence of 18-β-Gly-PLGA or empty NP (final concentration of 5 µM) underwent incubation for 24 h under 5% $CO_2$. Following earlier instructions, total RNA was extracted. After being gently washed twice in PBS, TRI reagent was used to lyse the cells, which were then collected in 1.5 mL Eppendorf tubes. To each tube 250 µL of chloroform was added before being pulse-vortexed for 5 seconds at room temperature. The tubes underwent a

15-minute (12,000x g) centrifugation at 4 °C after a 10-minute incubation at room temperature. After the aqueous phase was transferred into brand-new Eppendorf tubes, 500 µL of ice-cold isopropyl alcohol was added to precipitate the RNA. The tubes underwent pulse-vortexing (for 5 s) and 10 minutes incubation period at room temperature. After being pulse-vortexed once more, the tubes were centrifuged for 10 minutes (12,000x g) at room temperature. The supernatant was decanted, and the RNA pellets were washed with 1 mL of 75% ethanol. Next, the tubes were centrifuged again at 8000x g for 5 minutes at 4 °C. Following another rinse, the RNA pellets were centrifuged at 8000x g for 5 minutes at 4 °C and then placed on ice to air-dry for 15 minutes after the ethanol was removed. Afterwards, nuclease-free water was used to resuspend the pellets. Using Nanodrop One (Thermo Fisher Scientific), the RNA purity and concentration were assessed. The cDNA was synthesized using reverse transcription of RNA. The mRNA levels of the target genes were assessed using qPCR [60]. The forward and reverse primers for *KRT18*, *EGFR*, *BRAF*, *KRAS, RIPK3, MLKL,* and *GAPDH* were procured from Merck (Table 1).



Table 1. The forward and reverse primers for *KRT18*, *EGFR*, *BRAF*, *KRAS* and *GAPDH.*

| Gene | Forward Primer | Reverse Primer |
|---|---|---|
| *KRT18* | GGAAGTAAAAGGCCTACAAG | GTACTTGTCTAGCTCCTCTC |
| *EGFR* | AGAAAGGCAGCCACCAAATTAGCC | TTCCTGGCTAGTCGGTGTAAACGT |
| *BRAF* | TGCTTGCTCTGATAGGAAAATG | AGCATCTCAGGGCCAAAAT |
| *KRAS* | TTAACCTTATGTGTGACATGTTCTAA | AGAATGGTCCTGCACCAGTAA |
| *RIPK3* | AACTTTCAGAAACCAGATGC | GTTGTATATGTTAACGAGCGG |
| *MLKL* | GTGAAGAATGTGAAGACTGG | AAGATTTCATCCACAGAGGG |
| *GAPDH* | TCGGAGTCAACGGATTTG | CAACAATATCCACTTTACCAGAG |

**Proteome profiler human oncology array**

The proteins were extracted from A549 cells using RIPA buffer supplemented with protein inhibitor tablets (Roche Diagnostics, Basel, Switzerland) after 24 hours of treatment with or without 18-β-Gly-PLGA or empty NP. Using a Pierce BCA protein assay kit (Thermo Fisher), the bicinchoninic acid (BCA) assay used to measure the protein. The ChemDoc MP imaging device (Bio-Rad, Hercules, CA, USA) was used to take pictures of the protein signals in the array. The protein signals' pixel densities were examined using Image J software (version 1.53c, Bethesda, MD, USA) [24].

**Annexin V-FITC immunofluorescence**

For the study of 18-β-Gly-PLGA induced apoptosis of A549 cells, we performed the Annexin V-FITC staining and microscopic imaging. The cells were grown in a cover slip inside a 6 well plated and treated for 24 hours with or without 18-β-Gly-PLGA or empty NPs and stained with Annexin V-FITC as describe previously [61]. Microscopic image of stained cells was taken with a fluorescence microscope [61] (Zeiss Axio Imager Z2).

**Statistical analysis**

The results of experiments were reported as mean ± SEM values and carried out in triplicate. Using a two-tailed Student's t test, the statistical significance between the two groups were compared. The analysis of data from more than two groups was undertaken using one-way ANOVA and the GraphPad Prism software (version 9.5.1.1). At $P<0.05$, statistical significance was recognized.

## 3. RESULTS

**Preparation and physiochemical characterisation of 18-β-Gly-PLGA formulation**

The wavelength for 18-β-Gly was discovered to be 248nm based on the solubility analysis. A concentration versus absorbance study was performed and showed that the absorbance grew linearly as a function of concentration (Figure 1). The graph yielded the linear equation y = 0.03x + 0.0594 with an R2 value of 0.9714, indicating a significant and strong association between concentration and absorbance at 248 nm. Both empty NP and 8β-Gly-PLGA NPs had particle sizes under 200 nm.

18-β-Gly-PLGA was found to have a mean diameter of 136.2±3 nm, and all formulations while being negatively charged at -2.76, also displayed a narrow PDI of 0.298. The 18-β-Gly-PLGA formulation showed a good entrapment effectiveness of 60.23±0.13%. The SEM micrograph reveals that the 18-β-Gly-PLGA nanoparticles are generally spherical with smooth surfaces (Figure 2a). Notably, the morphological size observed in the SEM image appears larger than the hydrodynamic size. This size difference is likely due to the nanoparticles being hydrated and swollen by residual water, causing them to expand in the micrograph. Furthermore, the *in vitro* release study indicates that 18-β-Gly-PLGA nano-formulation able to show sustained release. In contrast, free 18-β-Gly exhibits complete release within just 3 hours, as shown in Figure 2b. 18-β-Gly-PLGA nano-formulation showed a pattern of an initial burst release which later plateaued around 14%.

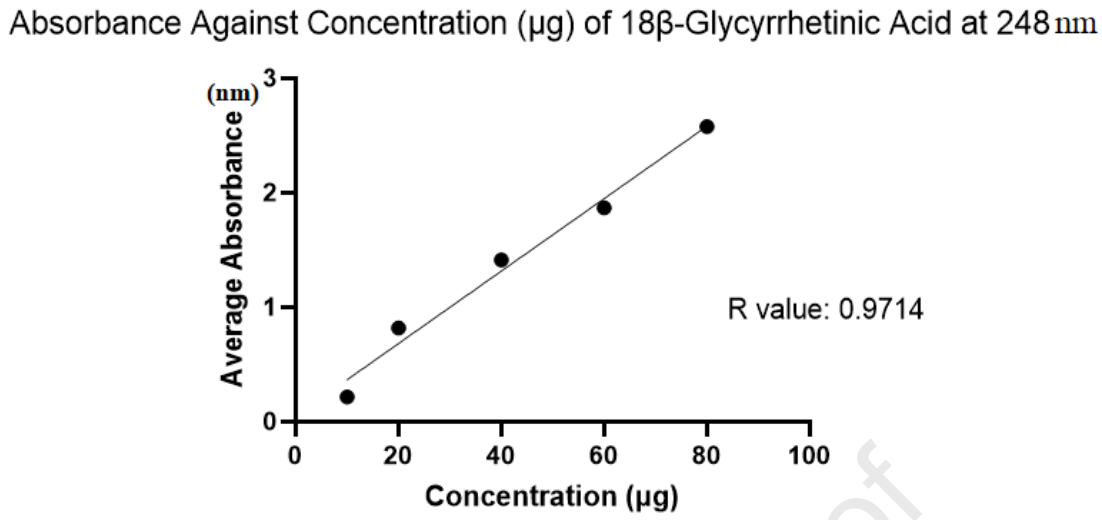


**Figure 1.** Graph of absorbance against concentration (µg) of 18-β-Gly. The graph shows significant and strong association between concentration and absorbance at 248 nm.

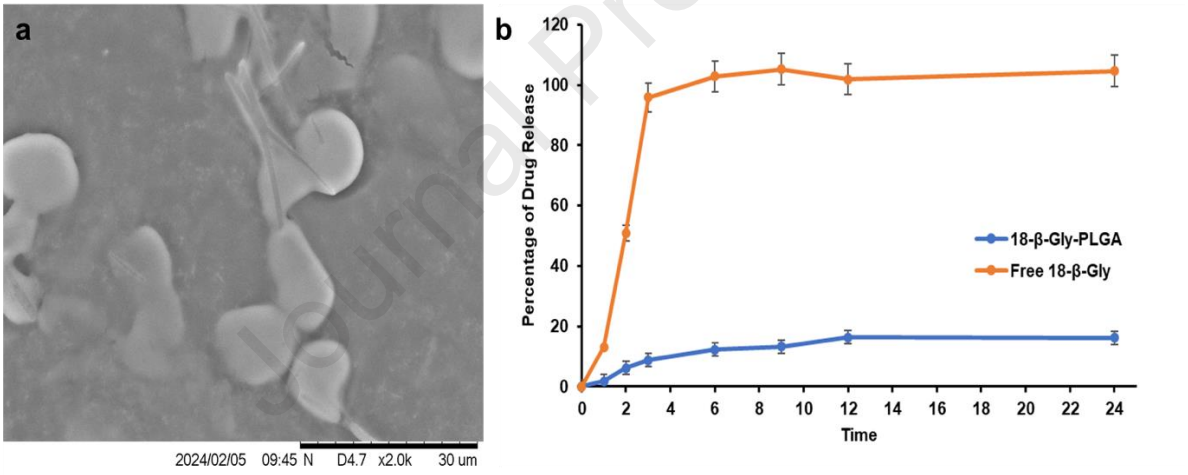


**Figure 2.** a. SEM image of 18-β-Gly-PLGA nanoparticles. b. *In vitro* release study of free 18-β-Gly (control) and 18-β-Gly-PLGA nanoparticles.

**Antiproliferative activity of 18-β-Gly-PLGA and empty NP on A549 cell proliferation**

18-β-Gly-PLGA showed a significant dose-dependent reduction in A549 cell proliferation. At a concentration of 2.5 µM, 18-β-Gly-PLGA significantly inhibited cellular proliferation by approximately15% (Figure 3, $p<0.0001$ vs control). A 20-fold increased (50 µM) dose of 18-

β-Gly-PLGA inhibited cell proliferation by 50% compared to the control (Figure 3, $p<0.0001$). Empty NP did not have a significant inhibitory effect against A549 cell proliferation. For subsequent experiments, 5 μM of 18-β-Gly-PLGA and empty NP were used for A549 cell line as 5 μM was the maximum safe dose for maintaining healthy human broncho epithelial cells i.e., BEAS-2B cell line.

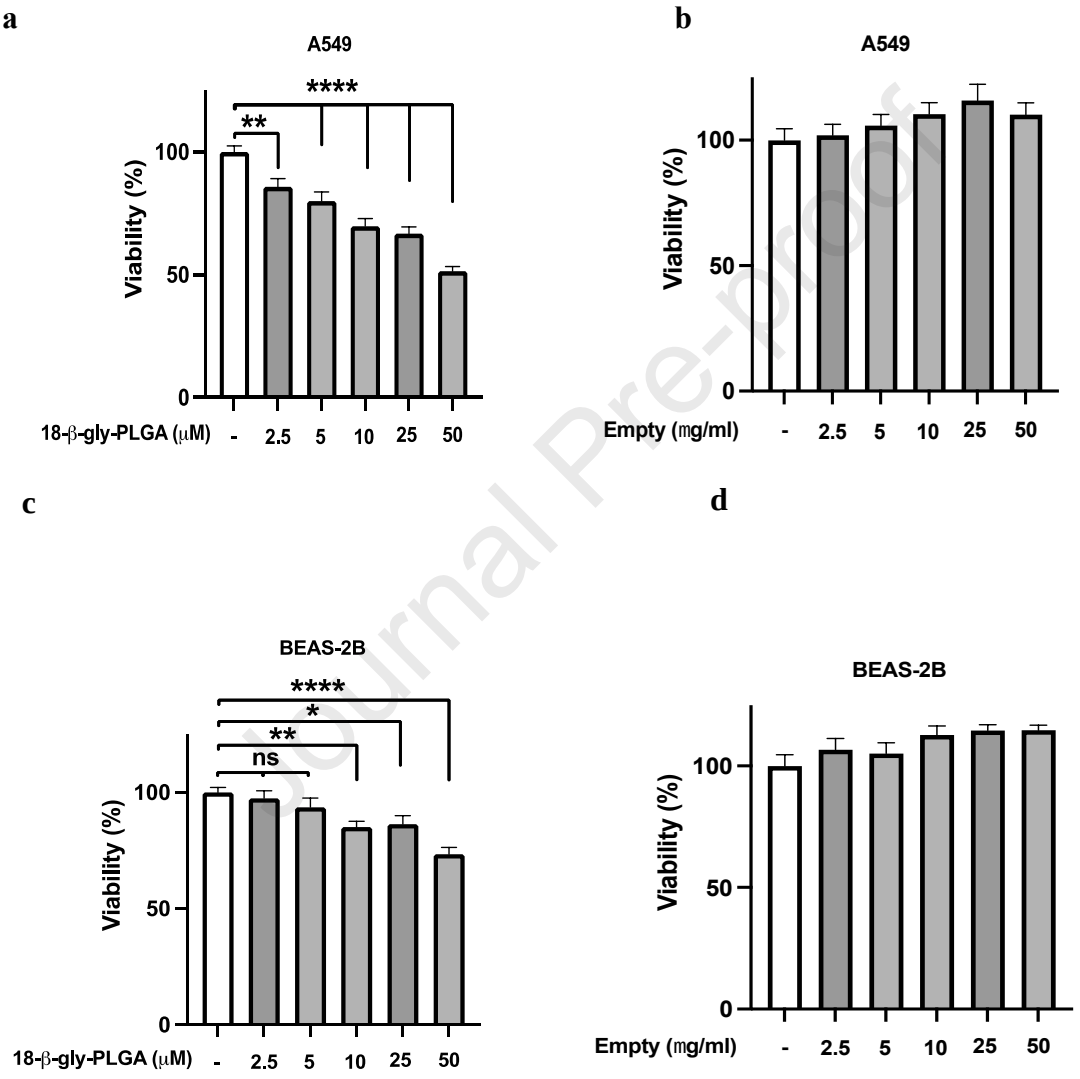


**Figure 3.** Anti-proliferative effects of 18-β-Gly-PLGA and empty NP in A549 cells and BEAS-2B cells. (Panel a and b) A549 cells and (Panel c and d) BEAS-2B cells were treated with or without 18-β-Gly-PLGA (0, 2.5, 5, 10, 25 or 50 μM) or empty NP (0, 2.5, 5, 10, 25 or 50 μM) for 24 h, followed by incubation with MTT. The purple formazan crystals formed were dissolved with DMSO and the absorbance was measured with microplate reader. The data in

the figure are mean ± SEM of four independent experiments. ****p<0.0001. The nano-formulation showed significant dose-dependent reduction in A549 cells proliferation. The nano-formulation began to significantly inhibit A549 cells proliferation starting from 2.5 µM with a percent inhibition of around ~15% and cell proliferation inhibition by the nano-formulation increased up to ~50% at doses of 50 µM. The maximum safe dose concentration for the nano-formulation against healthy broncho-epithelial cell determined to be 5 µM.

**Anti-colony formation activity of 18-β-Gly-PLGA and empty NP in A549 cells**

When compared to the empty NP, the crystal violet staining of the A549 cell colonies clearly demonstrates the anti-proliferative action of 18-β-Gly-PLGA (5 µM) (Figure 4). The representative well photos of 6-well plates clearly show a substantial reduction in the number of cell colonies in 18-β-Gly-PLGA treated cells, compared to empty NP (Figure 4).

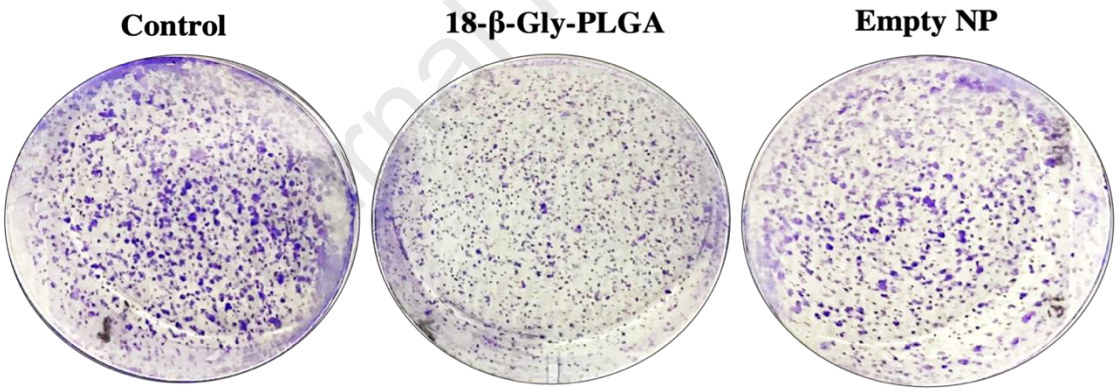


**Figure 4**. Effect of 18-β-Gly-PLGA and empty NP on colony formation of A549 cells. After seeding A549 cells in 6-well plate, they were cultured for two weeks in the absence or presence of 5 µM 18-β-Gly-PLGA or 5 µM empty NP. The cell colonies were stained with crystal violet and photographed. The figure shows representative images from four independent experiments. The representative well photos of 6-well plates clearly show substantial reduction in the number of cell colonies in 18-β-Gly-PLGA treated cells, compared to empty NP.

**Anti-migratory activity of 18-β-Gly-PLGA and empty NP in A549 cells**

Images from a wound healing assay revealed that the control and empty NP treated A549 cells showed no significant difference with regards to healing of the wound (Figure 5A). However, A549 cells treated with 18-β-Gly-PLGA at a dosage of 5 μM strongly inhibited wound closure (Figure 5A). With approximately 28% inhibition of wound closure 24 hours after treatment with 5 μM 18-β-Gly-PLGA compared to the control (Figure 5B, $p<0.05$), the quantification of percentage wound closure is comparable with Figure 5A.

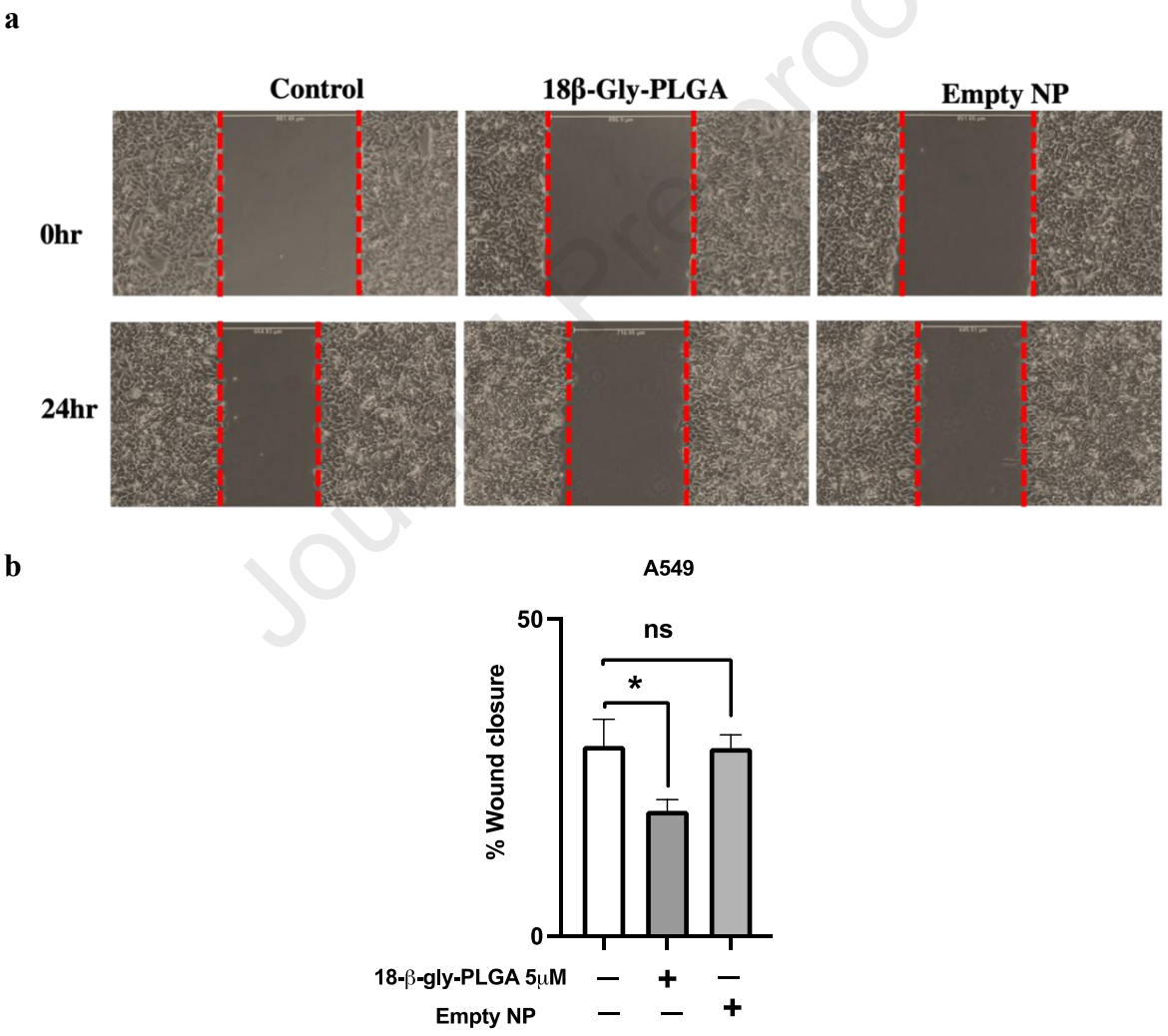


**Figure 5.** Effects of 18-Gly-PLGA and empty NP on wound healing in A549 cells. Using a phase contrast microscope at a 4x magnification, panel a shows the images taken at 0 and 24 hours after the start of the treatment. Panel b shows % wound closure after 24 hours of

incubation. Data in the Figure 5B is expressed as mean ± SEM of three independent experiments. *p<0.05. A549 cells treated with 18-β-Gly-PLGA at a dosage of 5 µM showed a strong inhibition of wound closure. Panel B showing around ~28% inhibition of wound closure by our nano-formulation, when compared to control.

**Anti-invasion activity of 18-β-Gly-PLGA and empty NP in A549 cells.**

A549 cells treated with 5µM 18-β-Gly-PLGA compared to the control and empty NP showed less cellular migration (Figure 6A). This is further supported by the fact that the migration was reduced by ~20% when treated with 18-β-Gly-PLGA at a concentration of 5 µM (Figure 6B, p<0.05 versus control).

**a**

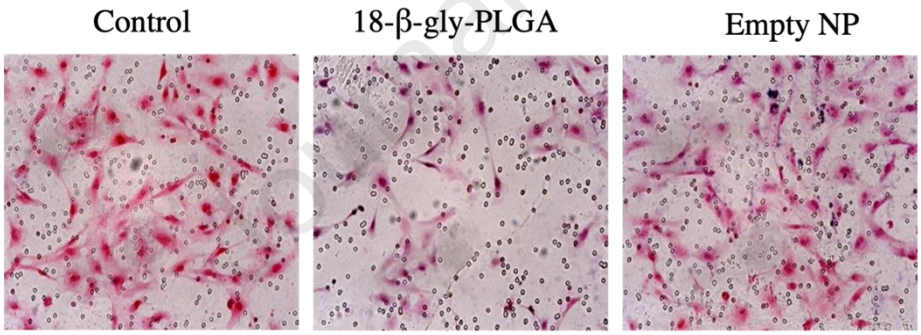


**b**

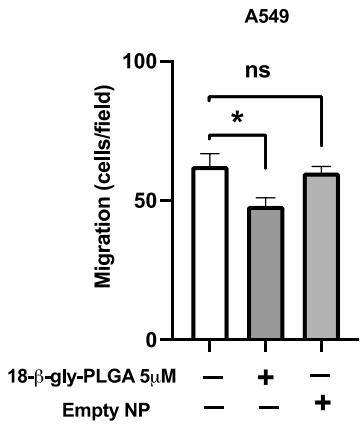

**Figure 6.** Effect of 18-β-Gly-PLGA and empty NP on migration of A549 cells in a trans-well chamber. The cells seeded in a trans-well chamber were treated with/without 5 μM 18-β-Gly-PLGA or 5 μM empty NP for 24 h to allow cell migration. Migrated cells in the lower compartment were stained with staining solution of haematoxylin and eosin and microscopic images were taken at 20X magnification. Figure 6A shows representative images from 4 independent experiments. Figure 6B shows the number of cells migrated/high power field. The data are expressed as mean ± SEM of 4 independent experiments. **p<0.01, ****p<0.0001. Panel a indicate A549 cells treated with the nano-formulation showed fewer of the cells migrated compared to empty nanoparticle. This is further supported by panel b showing cell migration was reduced by ~20% at cells treated with 5 μM 18-β-Gly-PLGA nano-formulation.

**Effects of 18-β-Gly-PLGA on *KRT18*, *EGFR*, *BRAF*, and *KRAS* mRNA expression**

Five μM of 18-β-Gly-PLGA significantly downregulated the transcription of the cancer proliferation and metastasis-associated genes *KRT18*, *EGFR*, *BRAF* and *KRAS* (Figure 7, *p<0.05, **p<0.01, ***p<0.001). In particular, a 43% reduction of *KRT18* in those cells treated with 18-β-Gly-PLGA compared to the untreated cells. Similarly, percentage of inhibition of *EGFR*, *BRAF* and *KRAS* in 18-β-Gly-PLGA treated cells was shown to be 19.3%, 14.8% and 13.7% respectively compared to untreated cells. Five μM of empty NP did not elicit these effects.

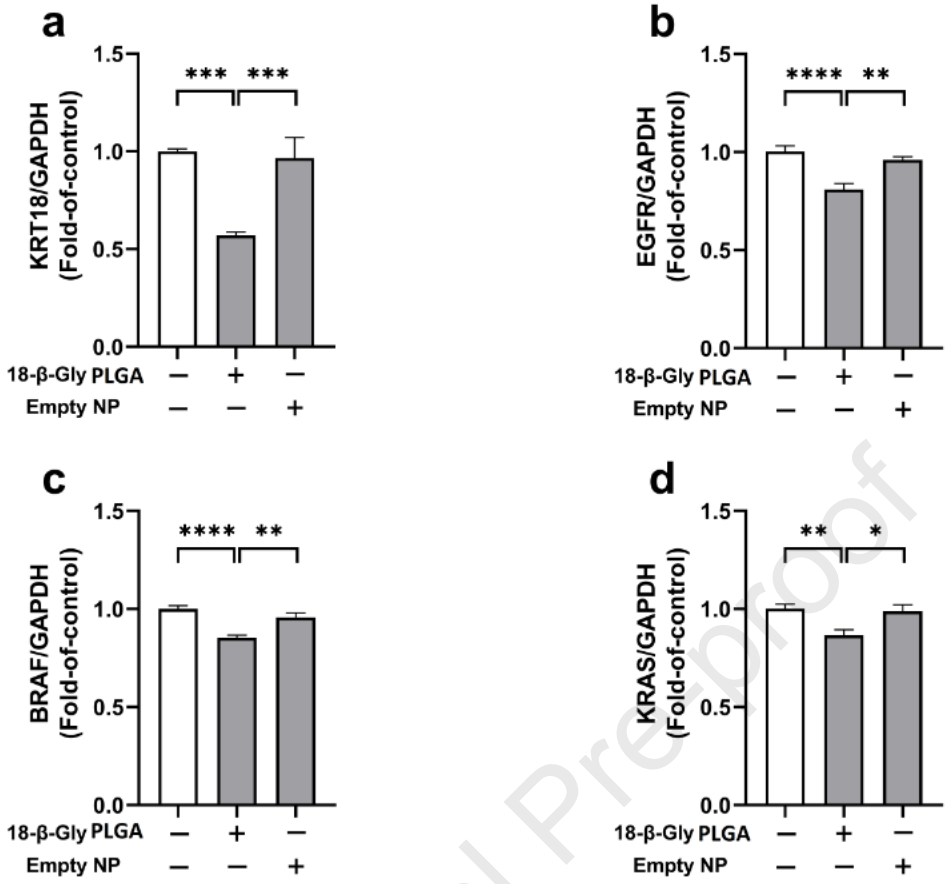


**Figure 7.** Regulation of mRNA levels *KRT18, EGFR,* BRAF and *KRAS* by 18-β-Gly-PLGA and empty NP. A549 cells were treated with 5 μM 18-β-Gly-PLGA, and 5 μM empty NP for 24 hours. The figure shows the mRNA levels of *KRT18* (Panel A), *EGFR* (Panel B), *BRAF* (Panel C) and *KRAS* (Panel D), normalised against the levels of *GAPDH*. Data are expressed as mean ± SEM of 3 independent experiments. *p<0.05, ***p<0.001, ****p<0.0001.

**Effects of 18-β-Gly-PLGA on expression of oncogenic proteins involved in cancer cell proliferation, migration, and survival**

At 5 μM doses, the treatment of A549 cells with 18-β-Gly-PLGA significantly reduced the protein expression of ErbB2, HO-1/HMOX1, M-CSF, mesothelin, PDGF-AA, survivin and ENPP2-Autotaxin (Figure 8, *p<0.05 vs control). ErbB2 expression reduced by 36% in 18-β-Gly-PLGA treated cells compare to the control. Similarly, HO-1/HMOX1, M-CSF, mesothelin, PDGF-AA, survivin and ENPP2-Autotaxin expression reduced by 14%, 33%, 31%, 30%, 10% and 25% respectively in 18-β-Gly-PLGA treated cells compare to untreated cells.

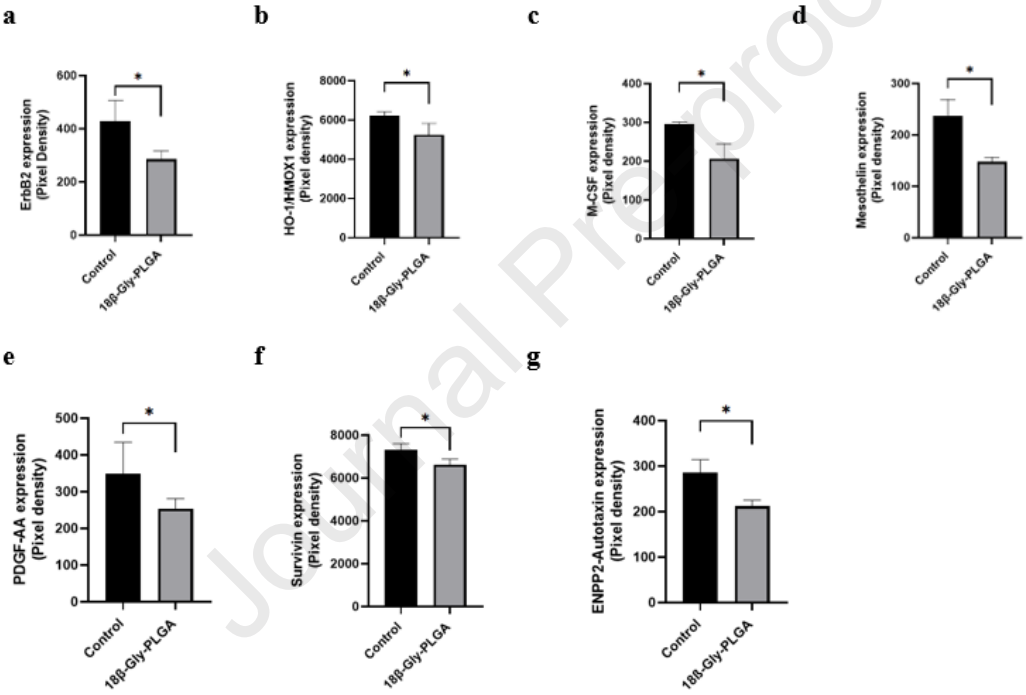


**Figure 8.** Regulation of protein expression involved in cancer cell proliferation and migration by 18-β-Gly-PLGA. After treatment of A549 cells with 5 μM 18-β-Gly-PLGA for 24 h, the proteins were extracted, and the expression of proteins associated with cell proliferation, migration, and survival was evaluated with Proteome Profiler Human XL oncology array kit. The figure shows the protein expression of ErbB2 (graph A), HO-1/HMOX1 (graph B), M-CSF (graph C), mesothelin (graph D), PDGF-AA (graph E), survivin (graph F) and ENPP2-Autotaxin (graph G). The data are expressed as mean ± SEM of 3 independent experiments.

*p<0.05. At 5 µM doses, the treatment of A549 cells with 18-β-Gly-PLGA significantly reduced the protein expression of ErbB2, HO-1/HMOX1, M-CSF, Mesothelin, PDGF-AA, Survivin and ENPP2-Autotaxin.

**18-β-Gly-PLGA induced apoptosis of A549 cells**

At 5 µM dose, the treatment of A549 cells with 18-β-Gly-PLGA significantly increased the staining Annexin V-FITC as shown in fluorescence microscopic image figure 9A and fluorescence quantification (figure 9B). Annexin V binds to phosphatidylserine on outer layer of apoptotic cells' phospholipid layer. Thus, strong intensity of Annexin-FICT in 18-β-Gly-PLGA group which is 1.9 fold greater (**p<0.01) compared to control A549 or empty NPs treated A549 suggests cells undergoing apoptosis more after treatment to 18-β-Gly-PLGA. This was further confirmed mechanistically with gene expression of key apoptosis/necroptosis gene. As shown in figure 9C and 9D, the expression of RIPK3, and MLKL was upregulated after 24hrs treatment of by 18-β-Gly-PLGA respectively in 18-β-Gly-PLGA treated cells compare to untreated cells and empty NP. However, statistically, only the expression of MLKL was significantly increased while there was an increasing trend (but not significant) of RIPK3 in 18-β-Gly-PLGA group compared to untreated control.



a

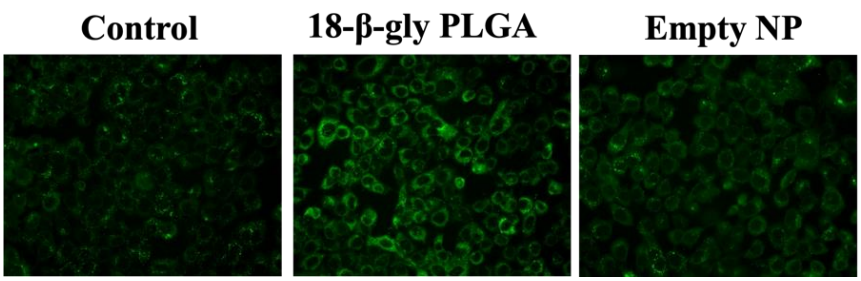


b

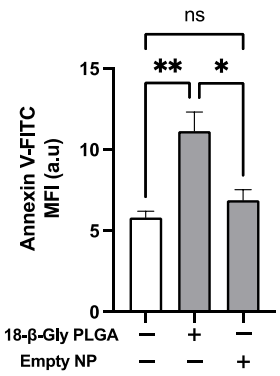

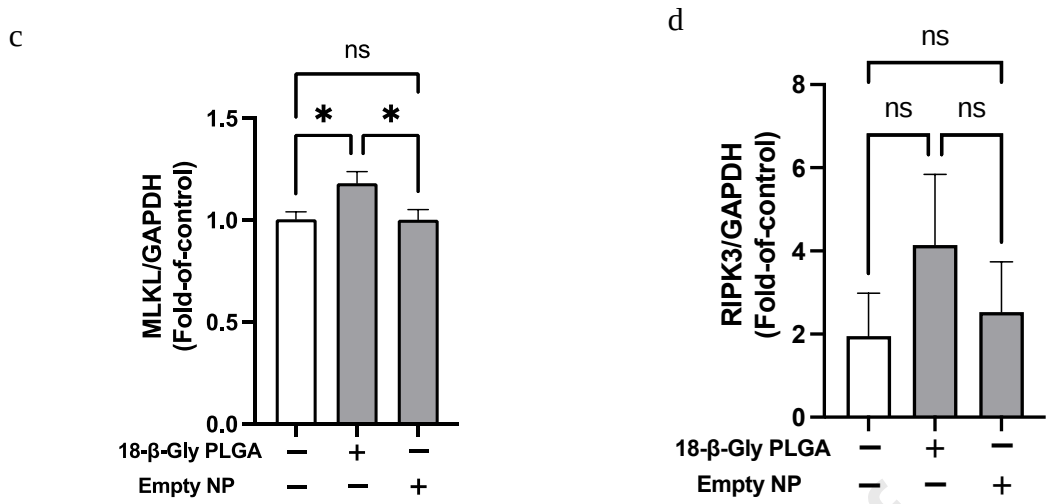


**Figure 9.** 18-β-Gly-PLGA induced apoptosis of A549 cells was measured by a) Annexin-V FITC fluorescence microscopic imaging of A549 cells treated with 5 μM 18-β-Gly-PLGA or empty NP for 24 h and b) quantification of fluorescence intensity in terms of mean fluorescence intensity (MFI) arbitrary unit (a.u) using ImageJ. mRNA levels *MLKL* (panel c), *RIPK3* (panel d), normalised against the levels of *GAPDH* in A549 cells after treatment of 18-β-Gly-PLGA or empty NPs was performed by qPCR. Data are expressed as mean ± SEM of 3 independent experiments. *$p<0.05$, **$p<0.01$ (18-β-Gly-PLGA vs untreated control).

## 4. Discussion

Lung cancer represents one of the most lethal cancers due to its high morbidity and mortality rates worldwide. Continuing research regarding therapeutic alternatives is crucial due to the fact that the current first-line medications for lung cancer has significant drawbacks such as high cost and unfavourable side effects. In light of this, research into diverse nutraceuticals or bioactive compounds from medicinal plants may provide better alternatives with increased efficacy against the disease. Many compounds have demonstrated biological activity, including anti-neoplastic effects [24, 30, 31, 34]. In our study, 18-β-Gly was chosen as a phytoceutical to evaluate whether it possesses anti-neoplastic activity against the A549 lung cancer cell line.

18-β-Gly has demonstrated its potential as a therapeutic agent against various diseases, however, there are certain challenges limiting its potential usage in a clinical setting, which include poor bioavailability and low water solubility [42]. To utilise 18-β-Gly for clinical purposes, it is necessary to develop a new drug delivery system using nanotechnology and advanced pharmacological approaches. Numerous studies have indicated that formulating 18-β-Gly with NP such as hyaluronic acid and liposomes help to improve the physicochemical properties of the compound [62-64]. NP-based pharmaceutical formulations can be prepared as a carrier for 18-β-Gly, thus, providing a more effective form of drug delivery systems. PLGA-based drug delivery systems provide versatility in designing and delivery of nutraceuticals to treat pulmonary diseases [50]. Several research studies have shown PLGA has the ability to improve the efficacy of anti-cancer agents compared to free anti-cancer agents [65, 66]. With a similar research hypothesis, we formulated and investigated 18-β-Gly-PLGA ability as an anti-cancer agent.

For this study, 18-β-Gly nano-formulation using PLGA based nanotechnology was successfully prepared by dissolving the compound into the PLGA and adding into the solubilizer Poloxamer 407. Lactic acid and glycolic acids are joined by ester bonds to form the biodegradable copolymer PLGA [50]. Due to its extensive clinical usage, favourable degradation processes and potential for prolonged drug delivery, PLGA is the most widely used biodegradable polymer. In particular, PLGA, approved by the FDA for use, is widely employed to provide regulated delivery systems for medicines and small compounds. Drug release at the desired concentration can be achieved by using PLGA breakdown [67]. Poloxamer 407 was used as it provides steric stabilization and outer surface coverage for dispersed colloidal particles [68].

PLGA typically has a mean diameter of 10 to 100 nm [50]. The mean diameter of 18-β-Gly-PLGA is 136.2±3 nm which is slightly bigger than empty PLGA NP. Additionally, it is

interesting to note the favourable physiochemical properties of our PLGA formulation. The PDI for the 18-β-Gly-PLGA had negative values of less than 0.5, indicating that the sample was generally more uniform and had low polydispersity [69]. A good entrapment efficiency of 60.23±0.13% was also noted for the 18-β-Gly-PLGA formulation. Entrapment efficiency is defined as the difference between the initial drug and free drug in the supernatant with respect to the total amount added to the nano-formulation. An important study for determining the effectiveness, safety, and quality of drug delivery systems based on NPs is the *in vitro* drug release study [70]. According to our findings, 18-β-Gly-PLGA demonstrated sustained medication release and lasted longer than 24 hours. This extended release is advantageous since it guarantees that patients will benefit from the safe drug dosage over a longer period of time and hence, subsequently reduces the frequency of drug usage.

After confirming the 18-β-Gly-PLGA complex possesses favourable characteristics *i.e.* particle size, PDI, entrapment efficiency and *in vitro* release, we investigated the *in vitro* biological activity of the formulation against human-derived cancer cells. Proliferation and migration/metastasis are the two primary processes in the development of lung cancer. The cell proliferation assays showed that at a dose of 5 μM, 18-β-Gly-PLGA significantly reduced A549 cell growth by approximately18% (Figure 3), while the empty NPs had zero effect against the A549 cells, thereby highlighting the anti-cancer effects of 18-β-Gly. The decrease in the cell growth was due to apoptosis of A549 after 24hrs treatment of 5 μM of 18-β-Gly-PLGA through upregulation of *MLKL* gene as shown in Figure 9C.

We observed that 18-β-Gly-PLGA significantly reduced A549 cellular wound closure in the scratch wound healing and trans-well chamber migration assays. Approximately 28% inhibition of wound closure was evident by in those cells treated with 5 μM of 18-β-Gly-PLGA (Figure 5). Furthermore, the 18-β-Gly-PLGA formulation reduced (~20%) A549 cell migration also at a concentration of 5 μM (Figure 6).

Successively, we examined the impact of our formulation on the expression of four known oncogenes: KRT18, EGFR, BRAF, and KRAS. Overexpression of gene KRT18 is positively linked with tumour invasion and metastasis in human cancer [71], while the EGFR gene has been shown to be crucial for encoding proteins that transmit growth factor, which signal to the cells to grow and divides. Overexpression of EGFR associated with cancer cell proliferation [10]. Further, its gene expression is upregulated in 60% of NSCLC cases [10]. BRAF belongs to the RAF kinase family and plays a vital role in cellular development, proliferation, and differentiation *via* the mitogen-activated protein kinase (MAPK) pathway. Mutated BRAF is an oncogene that leads to cancer cell proliferation [9]. The KRAS gene, also a member of the RAF family, is involved in cellular growth signalling [8], while an altered KRAS gene has been shown to be highly expressed in aggressive lung cancer [8]. In the qPCR assays, we found that 18-β-Gly-PLGA significantly reduced the expression of KRT18, EGFR, BRAF, and KRAS genes, hence indicating a potent anti-cancer effect compared to the NP control. (Figure 10 provides a diagrammatic summary of these results).

Further investigation using the protein array, we showed that 18-β-Gly-PLGA significantly down-regulates the proteins associated with cancer cell proliferation and migration such as ErbB2, HO-1/HMOX1, M-CSF, mesothelin, PDGF-AA, survivin and ENPP2-Autotaxin (Figure 9). ErbB2 belongs to the epidermal growth factor (EGF) family, and plays an important role in NSCLC proliferation [12]. HO-1 is overexpressed in lung cancer and its high level of expression is directly linked to an advanced stage of lung cancer [72]. M-CSF is a colony stimulating factor that induces lung cancer cell invasion [6]. High level expression of M-CSF and interleukin-34 by cancer cells implies that the tumour will be more highly aggressive, resulting in poor survival rates among lung cancer patients [14]. Mesothelin is a plasma membrane differentiation antigen that is highly expressed in a variety of human solid tumours including almost all mesotheliomas and 70% of lung cancers [15]. Mesothelin plays a crucial

role in regulating human lung cancer and mesothelioma cells' epithelial-to-mesenchymal transition (EMT), which is significant in transforming well differentiated epithelial cell to undifferentiated mesenchymal cells for tumorigenicity, including metastasis [15]. PDFG-AA is a vital autocrine regulator in lung cancer that stimulates VEGF expression, is a key mediator in cancer angiogenesis [16]. The survivin gene prevents tumour cells from undergoing apoptosis, thus promoting the survival of cancer cells [17]. ENPP2-Autotaxin is a glycoprotein that extracellularly, catalyses the synthesis of lysophosphatidic acid [7]. In lung cancer, the higher expression rate of ENPP2-Autoraxin noted in patients' biopsies and sera confirmed its' pro-carcinogenic role in lung cancer [7]. Down-regulation of these important cancer proliferation and migration proteins showcases the potential of 18-β-Gly-PLGA as a viable option for lung cancer treatment.

Luo et al conducted a study and showed that pure 18-β-Gly at a concentration of 10 μM was able to significantly reduce the viability of A549 cells [69]. Furthermore, a study by Huang et al, the authors demonstrated that at 160 μM [73], pure 18-β-Gly significantly decreased the percentage of viable A549 cells to 40.5±10.5%. Similarly, another study by Tang et al showed that pure glycyrrhetinic acid inhibited A549 cells line at 40 μM [74]. These two studies taken together, clearly highlights that our prepared nano-formulation at a lower concentration of 5 μM, was far superior with regards to the inhibition of A549 cell proliferation. Moreover, our results have clearly show that the 18-β-Gly formulation into PLGA offers significantly more pharmacological and biological advantages than 18-β-Gly alone.

Given that the majority of this work was based on *in vitro* analysis, future directions should include the additional testing of other cell lines, such as SCLC and NSCLC. Further research, to explore the therapeutic potential of 18-β-Gly in treating asthma and COPD should also be undertaken. Moreover, only four genes relevant to lung cancer were included in our

investigation and hence, other genes or proteins shown in Figure 10 should be evaluated regarding as to whether they too, are also downregulated by 18-β-Gly-PLGA.

To further research in this area, it would be beneficial to undertake an *in vivo* biological investigation of 18-β-Gly in the PLGA formulation using the inhaled administration method in an experimental mouse model in combination with other tested models. By using an animal model, the long-term safety, pharmacokinetics, herb-drug interactions, and a variety of other aspects could be assessed to help determine toxicity and bioavailability.

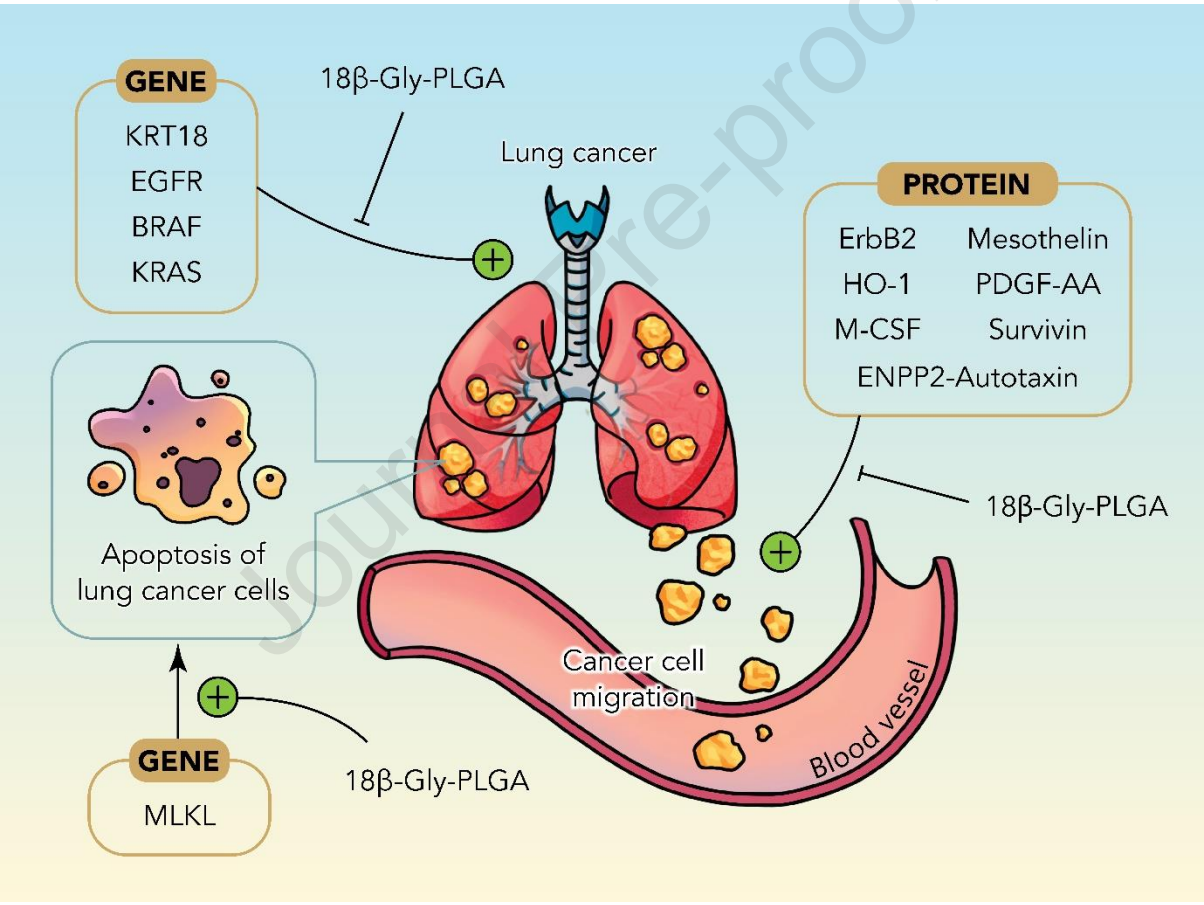


**Figure 10.** Underlying anti-cancer mechanism of 18-β-Gly-PLGA *in vitro* against A549 cells.

**Conclusion**

In our study, by controlling the mRNA expression of proto-oncogenes as well as down-regulating proteins associated with cancer cell proliferation and migration, 18-β-Gly-PLGA

was shown to exhibit strong anti-proliferative and anti-migratory effects in A549 cells. This work demonstrates the effective use of nanotechnology in the formulation of PLGA-encapsulated 18-β-Gly to produce greater efficacy and potency for the treatment of lung cancer compared to free 18-β-Gly. When combined with PLGA, 18-β-Gly offers far more pharmacological and biological advantages than free 18-β-Gly alone. The strong biological activities of 18-β-Gly-PLGA demonstrate its ability to outperform many of the disadvantages of pure 18-β-Gly through the nano-formulation process. With the aid of nanotechnology, this study will assist in focusing future research on the examination and development of 18-β-Gly as a viable anti-cancer medication therapy.

**Author Contributions**

Conceptualisation, D.K.C., K.D., and K.R.P; methodology, K.R.P., S.M., H.D., G.G., G.B.D., N.P. and T.M.; investigation, K.R.P., S.M., H.D., G.G., and G.B.D.; formal analysis, K.R.P., S.M., S.K.S., and G.B.D.; writing—original draft preparation, K.R.P.; S.M., and G.B.D., writing—review and editing, R.J.R., T.M., T.C., K.D., D.K.C., and P.M.H.; supervision, D.K.C., K.D. and P.M.H., funding acquisition, K.D., K.R.P., and D.K.C. All authors have read and agreed to the published version of the manuscript.



**Funding**

This project is supported by a research grant from the International Medical University, Malaysia, and University of Technology Sydney Australia Key Technology Partner Grant. (UTS-KTP grant).

**Acknowledgments**

The authors are thankful to the Graduate School of Health, University of Technology Sydney, Australia and the International Medical University, Malaysia for their support. KRP is supported by a fellowship from Prevent Cancer Foundation (PCF) and the International Association for the Study of Lung Cancer (IASLC). KD is supported by project grants from the Rebecca L Cooper Medical Research Foundation. Authors would also like to acknowledge

the funding support from Maridulu Budyari Gumal - The Sydney Partnership for Health, Education, Research and Enterprise (SPHERE) funding 2022 and 2023, Triple I CAG secondment/exchange grant-2023 and Triple I skills advancement grant-2023, University of Technology Key Technology Partnership (UTS-KTP) grant-2023.

## Conflicts of Interest

The authors declare no conflict of interest.

## References

1. Global Burden of Disease Cancer, C., et al., *Global, Regional, and National Cancer Incidence, Mortality, Years of Life Lost, Years Lived With Disability, and Disability-Adjusted Life-Years for 29 Cancer Groups, 1990 to 2017: A Systematic Analysis for the Global Burden of Disease Study.* JAMA Oncol, 2019. **5**(12): p. 1749-1768.
2. Malyla, V., et al., *Recent advances in experimental animal models of lung cancer.* Future Med Chem, 2020. **12**(7): p. 567-570.
3. Bray, F., et al., *Global cancer statistics 2018: GLOBOCAN estimates of incidence and mortality worldwide for 36 cancers in 185 countries.* CA Cancer J Clin, 2018. **68**(6): p. 394-424.
4. May, L., et al., *Sex Differences in Lung Cancer.* Cancers (Basel), 2023. **15**(12).
5. Kusnierczyk, P., *Genetic differences between smokers and never-smokers with lung cancer.* Front Immunol, 2023. **14**: p. 1063716.
6. Uemura, Y., et al., *Effects of GM-CSF and M-CSF on tumor progression of lung cancer: roles of MEK1/ERK and AKT/PKB pathways.* Int J Mol Med, 2006. **18**(2): p. 365-73.
7. Magkrioti, C., et al., *The Autotaxin-Lysophosphatidic Acid Axis Promotes Lung Carcinogenesis.* Cancer Res, 2018. **78**(13): p. 3634-3644.
8. Ghimessy, A., et al., *Current therapy of KRAS-mutant lung cancer.* Cancer Metastasis Rev, 2020. **39**(4): p. 1159-1177.
9. Roviello, G., et al., *Advances in anti-BRAF therapies for lung cancer.* Invest New Drugs, 2021. **39**(3): p. 879-890.
10. da Cunha Santos, G., F.A. Shepherd, and M.S. Tsao, *EGFR mutations and lung cancer.* Annu Rev Pathol, 2011. **6**: p. 49-69.
11. Weng, Y.R., Y. Cui, and J.Y. Fang, *Biological functions of cytokeratin 18 in cancer.* Mol Cancer Res, 2012. **10**(4): p. 485-93.
12. Landi, L. and F. Cappuzzo, *HER2 and lung cancer.* Expert Rev Anticancer Ther, 2013. **13**(10): p. 1219-28.
13. Kang, X., et al., *High glucose promotes tumor invasion and increases metastasis-associated protein expression in human lung epithelial cells by upregulating heme oxygenase-1 via reactive oxygen species or the TGF-beta1/PI3K/Akt signaling pathway.* Cell Physiol Biochem, 2015. **35**(3): p. 1008-22.
14. Baghdadi, M., et al., *High co-expression of IL-34 and M-CSF correlates with tumor progression and poor survival in lung cancers.* Sci Rep, 2018. **8**(1): p. 418.
15. He, X., et al., *Mesothelin promotes epithelial-to-mesenchymal transition and tumorigenicity of human lung cancer and mesothelioma cells.* Mol Cancer, 2017. **16**(1): p. 63.

16. Shikada, Y., et al., *Platelet-derived growth factor-AA is an essential and autocrine regulator of vascular endothelial growth factor expression in non-small cell lung carcinomas.* Cancer Res, 2005. **65**(16): p. 7241-8.
17. Hirano, H., et al., *Survivin expression in lung cancer: Association with smoking, histological types and pathological stages.* Oncol Lett, 2015. **10**(3): p. 1456-1462.
18. Ouyang, L., et al., *Programmed cell death pathways in cancer: a review of apoptosis, autophagy and programmed necrosis.* Cell Prolif, 2012. **45**(6): p. 487-98.
19. Liu, Z.G. and D. Jiao, *Necroptosis, tumor necrosis and tumorigenesis.* Cell Stress, 2019. **4**(1): p. 1-8.
20. Kannaujiya, V.K., et al., *Anticancer activity of NFκB decoy oligonucleotide-loaded nanoparticles against human lung cancer*. Journal of Drug Delivery Science and Technology, 2023. **82**: p. 104328.
21. Anand, U., et al., *Cancer chemotherapy and beyond: Current status, drug candidates, associated risks and progress in targeted therapeutics.* Genes Dis, 2023. **10**(4): p. 1367-1401.
22. Paudel, K.R., et al., *Targeting lung cancer using advanced drug delivery systems*, in *Targeting chronic inflammatory lung diseases using advanced drug delivery systems*. 2020, Elsevier. p. 493-516.
23. Alnuqaydan, A.M., et al., *Evaluation of the Cytotoxic Activity and Anti-Migratory Effect of Berberine-Phytantriol Liquid Crystalline Nanoparticle Formulation on Non-Small-Cell Lung Cancer In Vitro.* Pharmaceutics, 2022. **14**(6).
24. Paudel, K.R., et al., *Berberine-loaded liquid crystalline nanoparticles inhibit non-small cell lung cancer proliferation and migration in vitro.* Environ Sci Pollut Res Int, 2022. **29**(31): p. 46830-46847.
25. Mehta, M., et al., *Berberine loaded liquid crystalline nanostructure inhibits cancer progression in adenocarcinomic human alveolar basal epithelial cells in vitro.* J Food Biochem, 2021. **45**(11): p. e13954.
26. De Rubis, G., et al., *Involvement of osteopontin, EpCAM, estrogen receptor-alpha, and carbonic anhydrase IX protein in managing lung cancer via Berberine-loaded liquid crystalline nanoparticles.* Pathol Res Pract, 2023. **253**: p. 154971.
27. Malyla, V., et al., *Berberine nanostructures attenuate ss-catenin, a key component of epithelial mesenchymal transition in lung adenocarcinoma.* Naunyn Schmiedebergs Arch Pharmacol, 2023. **396**(12): p. 3595-3603.
28. Paudel, K.R., et al., *Cytotoxic mechanisms of berberine-phytantriol liquid crystalline nanoparticles against non-small-cell lung cancer.* EXCLI J, 2023. **22**: p. 516-519.
29. Hardwick, J., et al., *Targeting Cancer using Curcumin Encapsulated Vesicular Drug Delivery Systems.* Curr Pharm Des, 2021. **27**(1): p. 2-14.
30. Paudel, K.R., et al., *Rutin loaded liquid crystalline nanoparticles inhibit non-small cell lung cancer proliferation and migration in vitro.* Life Sci, 2021. **276**: p. 119436.
31. Wadhwa, R., et al., *Anti-inflammatory and anticancer activities of Naringenin-loaded liquid crystalline nanoparticles in vitro.* J Food Biochem, 2021. **45**(1): p. e13572.
32. Solanki, N., et al., *Antiproliferative effects of boswellic acid-loaded chitosan nanoparticles on human lung cancer cell line A549.* Future Med Chem, 2020. **12**(22): p. 2019-2034.
33. Kim, E., et al., *ROR activation by Nobiletin enhances antitumor efficacy via suppression of IkappaB/NF-kappaB signaling in triple-negative breast cancer.* Cell Death Dis, 2022. **13**(4): p. 374.
34. Manandhar, B., et al., *Zerumbone-incorporated liquid crystalline nanoparticles inhibit proliferation and migration of non-small-cell lung cancer in vitro.* Naunyn Schmiedebergs Arch Pharmacol, 2024. **397**(1): p. 343-356.

35. Alamil, J.M.R., et al., *Rediscovering the Therapeutic Potential of Agarwood in the Management of Chronic Inflammatory Diseases.* Molecules, 2022. **27**(9).
36. Paudel, K.R., et al., *In vitro anti-cancer activity of a polyherbal preparation, VEDICINALS(R)9, against A549 human lung adenocarcinoma cells.* Pathol Res Pract, 2023. **250**: p. 154832.
37. Mohamad, M.S.B., et al., *The versatility of 18ss-glycyrrhetinic acid in attenuating pulmonary inflammatory disorders.* EXCLI J, 2023. **22**: p. 188-190.
38. Ming, L.J. and A.C. Yin, *Therapeutic effects of glycyrrhizic acid.* Nat Prod Commun, 2013. **8**(3): p. 415-8.
39. Gumpricht, E., et al., *Licorice compounds glycyrrhizin and 18beta-glycyrrhetinic acid are potent modulators of bile acid-induced cytotoxicity in rat hepatocytes.* J Biol Chem, 2005. **280**(11): p. 10556-63.
40. Wang, L.J., et al., *Synthesis, biological evaluation and structure-activity relationships of glycyrrhetinic acid derivatives as novel anti-hepatitis B virus agents.* Bioorg Med Chem Lett, 2012. **22**(10): p. 3473-9.
41. Wang, L., et al., *The antiviral and antimicrobial activities of licorice, a widely-used Chinese herb.* Acta Pharm Sin B, 2015. **5**(4): p. 310-5.
42. Hao, J., et al., *Effect and mechanism of penetration enhancement of organic base and alcohol on glycyrrhetinic acid in vitro.* Int J Pharm, 2010. **399**(1-2): p. 102-8.
43. De Rubis, G., et al., *Applications and advancements of nanoparticle-based drug delivery in alleviating lung cancer and chronic obstructive pulmonary disease.* Naunyn Schmiedebergs Arch Pharmacol, 2023.
44. Saeid, A.B., et al., *Dissecting the in vitro fate of plant-derived bioactive encapsulated nanoparticles in lung diseases.* Food Bioscience, 2023: p. 103205.
45. Clarence, D.D., et al., *Unravelling the Therapeutic Potential of Nano-Delivered Functional Foods in Chronic Respiratory Diseases.* Nutrients, 2022. **14**(18).
46. Paudel, K.R., et al., *Nanomedicine and medicinal plants: Emerging symbiosis in managing lung diseases and associated infections.* EXCLI J, 2022. **21**: p. 1299-1303.
47. Chan, Y., et al., *Versatility of liquid crystalline nanoparticles in inflammatory lung diseases.* Nanomedicine (Lond), 2021. **16**(18): p. 1545-1548.
48. Khursheed, R., et al., *Expanding the arsenal against pulmonary diseases using surface-functionalized polymeric micelles: breakthroughs and bottlenecks.* Nanomedicine (Lond), 2022. **17**(12): p. 881-911.
49. Kaur, J., et al., *Polymeric micelles loaded with glyburide and vanillic acid: I. Formulation development, in-vitro characterization and bioavailability studies.* International Journal of Pharmaceutics, 2022. **624**: p. 121987.
50. Saxena, J., et al., *Targeting COPD with PLGA-Based Nanoparticles: Current Status and Prospects.* Biomed Res Int, 2022. **2022**: p. 5058121.
51. Gupta, M., et al., *A kNGR peptide-tethered lipid–polymer hybrid nanocarrier-based synergistic approach for effective tumor therapy: development, characterization, ex-vivo, and in-vivo assessment.* Pharmaceutics, 2022. **14**(7): p. 1401.
52. Kaur, J., et al., *Antidiabetic evaluation of vanillic acid-glyburide loaded polymeric micelles in high fat diet and streptozotocin induced diabetic rats.* 2023.
53. Hill, M., et al., *Formulation of Antimicrobial Tobramycin Loaded PLGA Nanoparticles via Complexation with AOT.* J Funct Biomater, 2019. **10**(2).
54. Abdelkader, D.H., et al., *A Novel Sustained Anti-Inflammatory Effect of Atorvastatin-Calcium PLGA Nanoparticles: In Vitro Optimization and In Vivo Evaluation.* Pharmaceutics, 2021. **13**(10).
55. Boltnarova, B., et al., *PLGA Based Nanospheres as a Potent Macrophage-Specific Drug Delivery System.* Nanomaterials (Basel), 2021. **11**(3).

56. Lin, C., et al., *Characterization and evaluation of hgf-loaded plga nanoparticles in a ccl4-induced acute liver injury mouse model.* Journal of Nanomaterials, 2019. **2019**: p. 1-13.
57. Astete, C.E. and C.M. Sabliov, *Synthesis and characterization of PLGA nanoparticles.* J Biomater Sci Polym Ed, 2006. **17**(3): p. 247-89.
58. Pereira, M.C., et al., *Effect of nanoencapsulation using PLGA on antioxidant and antimicrobial activities of guabiroba fruit phenolic extract.* Food Chem, 2018. **240**: p. 396-404.
59. Paudel, K.R., R. Karki, and D.-W. Kim, *Cepharanthine inhibits in vitro VSMC proliferation and migration and vascular inflammatory responses mediated by RAW264. 7.* Toxicology in vitro, 2016. **34**: p. 16-25.
60. Alnuqaydan, A.M., et al., *Phytantriol-Based Berberine-Loaded Liquid Crystalline Nanoparticles Attenuate Inflammation and Oxidative Stress in Lipopolysaccharide-Induced RAW264.7 Macrophages.* Nanomaterials (Basel), 2022. **12**(23).
61. Paudel, K.R., et al., *Rutin loaded liquid crystalline nanoparticles inhibit lipopolysaccharide induced oxidative stress and apoptosis in bronchial epithelial cells in vitro.* Toxicol In Vitro, 2020. **68**: p. 104961.
62. Nascimento, M.H.M.d. and D.R. de Araújo, *Exploring the pharmacological potential of glycyrrhizic acid: From therapeutic applications to trends in nanomedicine.* Future Pharmacology, 2022. **2**(1): p. 1-15.
63. Zhang, C., et al., *Glycyrrhetinic Acid Functionalized Graphene Oxide for Mitochondria Targeting and Cancer Treatment In Vivo.* Small, 2018. **14**(4).
64. Wang, X., et al., *Synthesis, characterization and liver targeting evaluation of self-assembled hyaluronic acid nanoparticles functionalized with glycyrrhetinic acid.* Eur J Pharm Sci, 2017. **96**: p. 255-262.
65. Xiong, B., et al., *Artesunate-loaded porous PLGA microsphere as a pulmonary delivery system for the treatment of non-small cell lung cancer.* Colloids Surf B Biointerfaces, 2021. **206**: p. 111937.
66. Roointan, A., et al., *A comparison between PLGA-PEG and NIPAAm-MAA nanocarriers in curcumin delivery for hTERT silencing in lung cancer cell line.* Cell Mol Biol (Noisy-le-grand), 2016. **62**(9): p. 51-6.
67. Chen, L., E. Mehrabi Nasab, and S.S. Athari, *Effect of Loaded Glycyrrhizic Acid on PLGA Nano-particle on Treatment of Allergic Asthma.* Iran J Allergy Asthma Immunol, 2022. **21**(1): p. 65-72.
68. Loo, Y.S., et al., *Encapsulation of berberine into liquid crystalline nanoparticles to enhance its solubility and anticancer activity in MCF7 human breast cancer cells.* Journal of Drug Delivery Science and Technology, 2020. **57**: p. 101756.
69. Danaei, M., et al., *Impact of Particle Size and Polydispersity Index on the Clinical Applications of Lipidic Nanocarrier Systems.* Pharmaceutics, 2018. **10**(2).
70. Weng, J., H.H.Y. Tong, and S.F. Chow, *In Vitro Release Study of the Polymeric Drug Nanoparticles: Development and Validation of a Novel Method.* Pharmaceutics, 2020. **12**(8).
71. Zhang, H., et al., *EGR1 decreases the malignancy of human non-small cell lung carcinoma by regulating KRT18 expression.* Sci Rep, 2014. **4**: p. 5416.
72. Degese, M.S., et al., *Expression of heme oxygenase-1 in non-small cell lung cancer (NSCLC) and its correlation with clinical data.* Lung Cancer, 2012. **77**(1): p. 168-75.
73. Huang, R.Y., et al., *18beta-Glycyrrhetinic acid suppresses cell proliferation through inhibiting thromboxane synthase in non-small cell lung cancer.* PLoS One, 2014. **9**(4): p. e93690.

74. Tang, Z.H., et al., *Glycyrrhetinic acid induces cytoprotective autophagy via the inositol-requiring enzyme 1alpha-c-Jun N-terminal kinase cascade in non-small cell lung cancer cells.* Oncotarget, 2015. **6**(41): p. 43911-26.

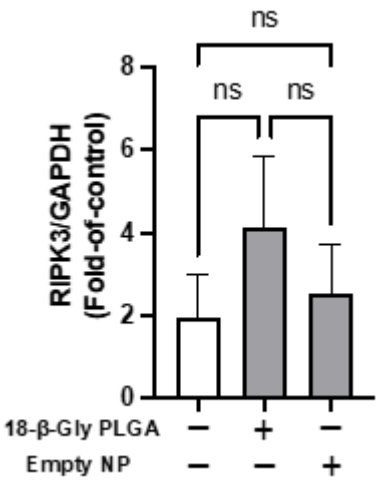

**Declaration of interests**

☒ The authors declare that they have no known competing financial interests or personal relationships that could have appeared to influence the work reported in this paper.

☐ The authors declare the following financial interests/personal relationships which may be considered as potential competing interests: